CATLOW, C. R. A. & JAMES, R. (1978). *Nature* (*London*), **272**, 603–605.
CATLOW, C. R. A. & JAMES, R. (1982). In *Chemical Physics of Solids and Their Surfaces*, Vol. 8, edited by J. M. THOMAS & M. W. ROBERTS, pp. 108–120. Spec. Period. Rep. London: Royal Society of Chemistry.
CATLOW, C. R. A. & MACKRODT, W. C. (1982). *Computer Simulation of Solids. Lecture Notes in Physics*, Vol. 166. Berlin: Springer.
CATLOW, C. R. A. & NORGETT, M. J. (1978). UKAEA Report AERE-M2936. United Kingdom Atomic Energy Authority.
CHEETHAM, A. K. & TAYLOR, J. C. (1977). *J. Solid State Chem.* **21**, 253–275.
CORMACK, A. N. (1982). In *Computer Simulation of Solids*, edited by C. R. A. CATLOW & W. C. MACKRODT. *Lecture Notes in Physics*, Vol. 166, ch. 20. Berlin: Springer.
CORMACK, A. N., JONES, R. M., TASKER, P. W. & CATLOW, C. R. A. (1982). *J. Solid State Chem.* **44**, 174–185.
DICK, B. G. & OVERHAUSER, A. W. (1958). *Phys. Rev.* **112**, 90–103.
FLETCHER, R. & POWELL, M. J. D. (1963). *Comput. J.* **6**, 163–168.
GREGSON, D., CATLOW, C. R. A., CHADWICK, A. V., LANDER, G. H., CORMACK, A. N. & FENDER, B. E. F. (1983). *Acta Cryst.* **B38**, 687–691..
JAMES, R. (1979). PhD Thesis, Univ. of London.
MARCHAND, R., BROHAN, L. & TOURNOUX, M. (1980). *Mater. Res. Bull.* **15**, 1129–1135.
PARKER, S. C., CATLOW, C. R. A. & CORMACK, A. N. (1984). *Acta Cryst.* **B40**, 200–208.
SLAUGHTER, M. (1966). *Geochim. Cosmochim. Acta*, **30**, 315–322.
THEOBALD, F., CABALA, R. & BERNARD, J. (1976). *J. Solid State Chem.* **17**, 431–439.
TIMOFEEVA, T. V., CHERNIKOVA, N. YU. & ZORKII, P. M. (1980). *Russ. Chem. Rev.* **49**, 966–997.
TOSI, M. (1964). *Solid State Physics*, edited by S. SEITZ & R. TURNBULL, Vol. 16, pp. 1–120. New York: Academic Press.

Acta Cryst. (1984). B40, 200–208

Structure Prediction of Silicate Minerals using Energy-Minimization Techniques

BY S. C. PARKER,* C. R. A. CATLOW AND A. N. CORMACK

Department of Chemistry, University College London, 20 Gordon Street, London WC1H 0AJ, England

(*Received 28 March 1983; accepted 5 December 1983*)

Abstract

Energy-minimization techniques are applied to the prediction of the structures of a range of silicate minerals. Interatomic potential models for silicates are developed, based on an ionic description. Such potentials are shown to yield accurate structures for olivines and for ring- and chain-structure silicates. No evidence is found for a large Si···Si short-range repulsion or for strong differences in the bonding of bridging and non-bridging oxygen ions. The calculations are also successful in predicting the effects of temperature and pressure on the structural parameters of garnets and olivines.

1. Introduction

In a recent study (Catlow, Cormack & Theobald, 1984) we showed that energy-minimization procedures could accurately predict the structures of a number of transition-metal oxides. In the present paper we apply these techniques to the study of silicate minerals. The work is motivated by the enormous diversity of silicate structural chemistry, and the valuable rôle which could be played by reliable theoretical methods in rationalizing and predicting structural variations within this class. An additional incentive for theoretical work is provided by the importance, in geophysical contexts, of knowledge of the structure and properties of minerals, often relating to conditions where reliable experimental data cannot be collected.

Central to the area of structure prediction of minerals by minimization procedures is the question of bonding and interatomic potentials in these systems. A large amount of work has been devoted to this problem (see, for example, Gibbs, 1982; Pauling, 1980; O'Keeffe & Hyde, 1978; Baur, 1972). Our approach, which is amplified in § 2, is based on the ionic model description; and, while we are well aware of the limitations in such models when applied to silicates, one of the main conclusions of this paper is that these models provide at least a basis for an acceptable description of the interaction potentials in silicate minerals.

The compounds examined in this paper contain either isolated SiO_4 groups or silicate rings and chains. Details of the results of applying minimization techniques to these systems are presented in § 3 after the description of techniques and potentials that is given below.

2. Simulation methods and interatomic potentials

The basic principle of our method is simple. As discussed by Catlow *et al.* (1984), calculation of the crystal energy of the structure under investigation is

---

* Present address: Department of Physical Chemistry, University of Cambridge, Lensfield Road, Cambridge CB2 1EP, England.

0108-7681/84/030200-09$01.50

combined with efficient minimization procedures. The lattice-energy calculation uses the technique described by Catlow & Mackrodt (1982); the Coulomb terms are handled by the Ewald transformation, while short-range terms are summed directly in real space.* The minimization methods employed a Newton–Raphson procedure (see Catlow & Mackrodt, 1982; Norgett & Fletcher, 1970) where practicable. In the case of the garnet structures discussed in § 3.4, the computer memory requirements for the matrix method exceeded those available, and a conjugate gradient technique (see Fletcher & Reeves, 1964) was used. Minimization may be carried out with respect to atomic coordinates with fixed cell dimensions or, alternatively, all structural parameters including the cell dimensions may be allowed to vary. The former is much less costly in computer time; moreover, cell dimensions are normally known with high accuracy even for compounds where only poor structural information is available. The work reported in this paper used, therefore, observed cell dimensions, although in a limited number of cases full energy minimizations were performed in order to confirm that our potentials generated the measured cell parameters with reasonable accuracy.

All calculations used the *METAPOCS* code (see Catlow *et al.*, 1984; Parker, 1983) which has been specifically written for crystal-structure simulations. The program requires as input firstly a 'trial' structure, which for silicates was generally an 'ideal' structure, as discussed below. Secondly, interatomic potentials must be specified. Our models for silicate systems will now be described.

Our potential model has two components: firstly, integral charges are assigned to each ion; secondly, we specify short-range-interaction terms that act between the centres of neighbouring ions and describe the effects of the overlap of the electron charge clouds. We should note that the SiO_4 group was not constrained as a rigid entity as in previous energy-minimization studies of olivines (Matsui & Matsumoto, 1982); and calculations of Miyamoto & Takeda (1980) and Matsui & Matsumoto (1982) have found that ionic-model potentials can successfully rationalize structural properties of olivines. Ionic polarizibility can be included but we have found that this generally causes only very small perturbations to the perfect-crystal structure, although such terms are of considerable importance in defect simulations (Catlow & Mackrodt, 1982).

The use of the ionic model for silicates is clearly an approximation; SiO_2 unquestionably has a large component of covalent bonding (Stewart, Whitehead & Donnay, 1980; Pauling, 1980; Tossel, 1977). However, there is evidence (Sasaki, Fujino & Takéuchi, 1979; Sasaki, Fujino, Takéuchi & Sadanaga, 1980) from X-ray diffraction studies that the bonding in silicates is appreciably more ionic. Moreover, we should emphasize that the use of ionic-model *potentials* does not necessarily imply that *electron density* distributions correspond to a fully ionic description; indeed, we can distinguish between ionicity when used as a description of interatomic forces and when used as a model for electron distribution; a point made originally by Cochran (1961) and discussed in greater detail by Catlow & Stoneham (1983). In addition, Jenkins (1982) and Jenkins & Hartman (1979) have shown that electrostatic calculations based on formal ionic charges can provide quantitative information on cohesion and structure in silicates. We are encouraged therefore to use the ionic model, at least as a starting point, for modelling interatomic forces in silicate minerals.

The general procedure that we adopted for evaluating parameters describing the short-range interactions in complex oxides was to transfer the relevant parameters derived from the simple oxides. However, this was only partly possible for silicate minerals because we could not evaluate a suitable potential model for α-quartz (SiO_2). Thus it was essential to devise an alternative scheme. The procedure was as follows: firstly, we transfered the parameters for all short-range interactions except those including silicon (*i.e.* Si···Si and Si···O interactions) from simple oxides (Mackrodt & Stewart, 1979; Catlow, 1977). We then derived parameters for the Si···Si and Si···O potentials such that the structural properties of selected systems could be reproduced. This scheme utilizes the abundance of silicate minerals and the low symmetry that is observed in many of their structures, as a result of which many different Si···O bond lengths may be sampled. Hence, the structures themselves contain considerable information on potentials.

We did include, at least initially, the short-range components of the Si···Si interaction because of speculation as to its significance (O'Keeffe & Hyde, 1978), but we found that its effect on the final calculated coordinates was negligible. The compounds whose structures were used in determining the potential parameters are listed in Table 1. We should emphasize that none of these structures have been used in our subsequent energy-minimization studies.

Initially we fitted the Si···O parameters for each structure in Table 1. However, we found that the parameters for all structures which contain isolated SiO_4 groups were similar, and the parameters for all structures based on silicate rings and chains were also similar; but there were significant differences between the parameters for the two structural groups. Thus, we averaged the parameters for each structural type to give two sets of potentials. The minimum-energy structure for all the compounds in Table 1 was then

---

* Summations of the short-range energies are truncated at an interatomic spacing after which they may be taken as negligible; in the present calculations a 'cut-off' of 15 Å was used.

Table 1. *Mineral structures used in fitting short-range parameters for silicon···oxygen interaction*

Name	Formula unit
Monticellite	$CaMgSiO_4$
Sillimanite	Al_2SiO_5
Titanite	$Ca(TiO)SiO_4$
Benitoite	$BaTi(SiO_3)_3$
Jadeite	$NaAl(SiO_3)_2$
β-Wollastonite	$CaSiO_3$

calculated using the appropriate potential. In every case the maximum discrepancy in the atomic positions was within three times the experimentally reported r.m.s. displacements due to thermal motion for the particular atom; we feel that such discrepancies are acceptable given that our simulations omit any representation of thermal motion.

3. Results

The structures investigated are listed in Table 2, where they are classified according to the nature of the silicate sublattice. The results of the minimization studies on each class of silicate are now discussed, after which we describe studies of the effects of temperature and pressure on structural parameters, the results of which give further insight as to the validity of our interatomic potentials.

3.1. *Structures with isolated* SiO_4 *tetrahedra*

Two types of silicate mineral are considered here, namely the olivine and zircon structures:

A. Olivine. The olivine structure of general formula M_2SiO_4 was first determined by Bragg & Brown (1926) and is based on a hexagonally close-packed oxygen sublattice with an orthorhombic unit cell. The structure has six distinct sites: three of these contain oxygen; there is one tetrahedral silicon site; the remaining two sites are octahedral and are occupied by divalent cations. We considered three compounds, namely Mg_2SiO_4, Fe_2SiO_4 and Mn_2SiO_4. Their structures have been determined recently (Fujino, Sasaki, Takéuchi & Sadanaga, 1981) using single-crystal X-ray diffraction techniques.

In all these compounds, the starting configuration for the minimization studies was the 'ideal' structure in which there is no distortion of the oxygen sublattice from the regular close-packed structure. One of the main aims of the calculations was to test the extent to which energy-minimization studies could reproduce the observed distortions of the structure from the ideal models. We found that, on minimization of the lattice energy, planes of oxygen ions rumple as the component polyhedra distort, see Fig. 1; this is exactly the distortion that is observed experimentally. A comparison of the observed and calculated atomic coordinates is given in Table 3. The good agreement shows that the distortions are correctly modelled. We note that the divalent cation coordinates are almost exactly predicted whilst larger discrepancies occur with the silicon positions. However, these differences are still, in general, less than three times the magnitudes of the temperature factors, which as argued above is a reasonable estimate of the maximum discrepancy.

Table 2. *Structures studied in this work*

A Orthosilicates		
Olivines	Mg_2SiO_4	Forsterite
	Fe_2SiO_4	Fayalite
	Mn_2SiO_4	Tephroite
Zircons	$ZrSiO_4$	Zircon
	$HfSiO_4$	Hafnon
	$ThSiO_4$	Thorite
	$USiO_4$	Coffinite
Garnets	$Mg_3Al_2Si_3O_{12}$	Pyrope
	$Ca_3Al_2Si_3O_{12}$	Grossular
B Ring silicates		
Three-membered rings	α-$SrSiO_3$	
	$Na_2Be_2Si_3O_9$	
Six-membered rings	$Al_2Be_3Si_6O_{18}$	Beryl
C Chain silicates		
Orthopyroxenes	$MgSiO_3$	Enstatite
	$FeSiO_3$	Ferrosilite
	Na_2SiO_3	Sodium metasilicate

B. Zircon structures. This class of mineral includes zircon itself ($ZrSiO_4$) (Hazen & Finger, 1979), thorite, $ThSiO_4$, and uranium silicate, $USiO_4$. The zircon structure also contains isolated silicate tetrahedra with zirconium being eightfold coordinated by the oxygen sublattice. The structure is tetragonal with the zirconium and silicon ions occupying special sites as shown in Fig. 2. We found that on minimization from a number of different initial configurations, the special sites were the most stable positions for both zirconium and silicon ions. Both sets of ions were displaced to ensure that the configuration was not in a metastable local minimum. As the cations reside on special sites we give in Table 4 a comparison of oxygen coordinates only. There is excellent agreement between the experimental and calculated values.

We repeated the procedure for hafnon ($HfSiO_4$) and compared the calculated minimum-energy structure with the results of a recent experimental study (Speer & Cooper, 1982). The structure of hafnon is similar to that of zircon, a fact which is consistent with the similarity of the ionic radii of Hf^{4+} and Zr^{4+}. Indeed, these two compounds are known to coexist in natural samples. The results in Table 4 show that we can model the differences between the two structures correctly.

Next we calculated the atomic coordinates for compounds containing the actinide ions: thorium and uranium. Again, we found that the agreement was good, particularly with the recent redetermination of thorite by Taylor & Ewing (1978). In accord with the observations of Speer & Cooper (1982), the *z* coordi-

Table 3. *Comparison of experimental and calculated fractional atomic coordinates for* Mg, Fe *and* Mn *olivines*

		Mg_2SiO_4		Fe_2SiO_4		Mn_2SiO_4	
		Experimental	Calculated	Experimental	Calculated	Experimental	Calculated
M(1)	*x*	0·0	0·0	0·0	0·0	0·0	0·0
	y	0·0	0·0	0·0	0·0	0·0	0·0
	z	0·0	0·0	0·0	0·0	0·0	0·0
M(2)	*x*	0·99169	0·99323	0·98598	0·98938	0·98792	0·98865
	y	0·27739	0·28481	0·28026	0·28562	0·28041	0·28580
	z	0·25	0·25	0·25	0·25	0·25	0·25
Si	*x*	0·42645	0·45655	0·43122	0·45437	0·42755	0·45359
	y	0·09403	0·10909	0·09765	0·11086	0·09643	0·10952
	z	0·25	0·25	0·25	0·25	0·25	0·25
O(1)	*x*	0·76594	0·76914	0·76814	0·74837	0·75776	0·74741
	y	0·09156	0·09442	0·09217	0·09888	0·09363	0·09731
	z	0·25	0·25	0·25	0·25	0·25	0·25
O(2)	*x*	0·22164	0·20747	0·20895	0·17983	0·21088	0·18338
	y	0·44705	0·44018	0·45365	0·47113	0·45369	0·47166
	z	0·25	0·25	0·25	0·25	0·25	0·25
O(3)	*x*	0·27751	0·29382	0·28897	0·29781	0·28706	0·30436
	y	0·16310	0·16270	0·16563	0·16626	0·16384	0·16579
	z	0·03304	0·04429	0·03643	0·05581	0·04140	0·05827
	a (Å)	4.7534		4·8195		4·9023	
	b (Å)	10·1902		10·4788		10·5964	
	c (Å)	5·9783		6·0873		6·2567	

nate of the oxygen sublattice does increase with cation size, which is due to the displacement of the oxygen sublattice perpendicular to the nearest-neighbour cation–cation separations. We also notice from Table 4 that the differences between the experimental (Fuchs & Gebert, 1958) and calculated values for uranium silicate are large in the *z* direction, although this is within the possible errors in our calculations due to the omission of thermal motion described above. However, the discrepancies may occur because there has been no recent redetermination of this structure, and we suggest that re-examination of the structure would be of value. Moreover, the success of these

Table 4. *Zircons: comparison of experimental and calculated fractional atomic coordinates (oxygen positions only)*

		Calculated	Experimental
$ZrSiO_4$	*x*	0·0	0·0
	y	0·0763	0·0660
	z	0·1776	0·1776
$HfSiO_4$	*x*	0·0	0·0
	y	0·0763	0·0655
	z	0·1937	0·1948
$ThSiO_4$	*x*	0·0	0·0
	y	0·0846	0·0732
	z	0·2047	0·2104
$USiO_4$	*x*	0·0	0·0
	y	0·0820	0·070
	z	0·2065	0·222

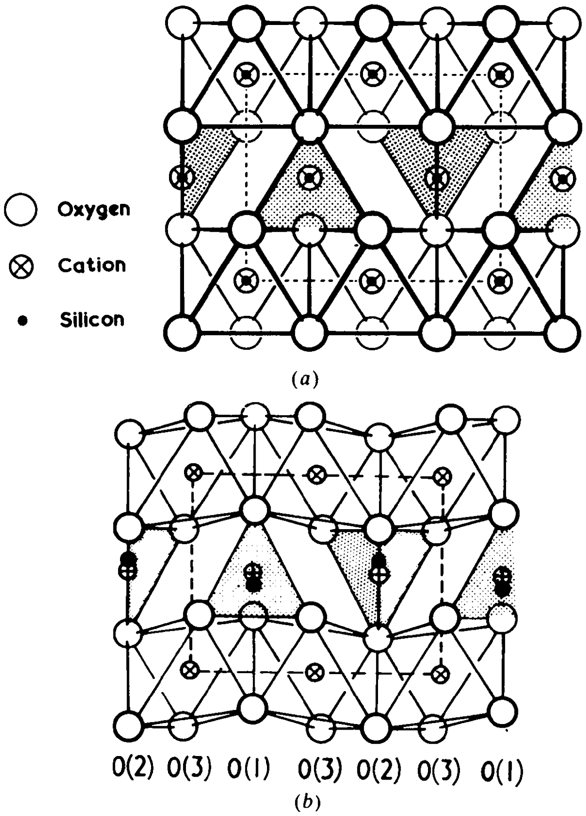

(*a*)

(*b*)

Fig. 1. The (*a*) idealized and (*b*) equilibrated structures of olivine.

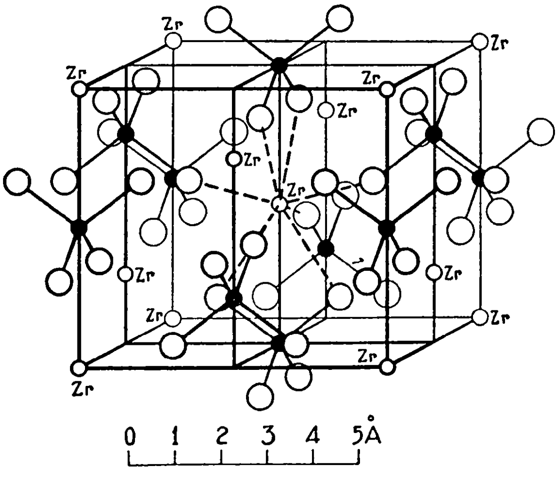

Fig. 2. The structure of zircon ($ZrSiO_4$).

Table 5. *The calculated and experimental fractional ionic coordinates of two silicates with three-membered rings*

(*a*) α-$SrSiO_3$
$a = 12·323$, $b = 7·139$, $c = 10·873$ Å, $\beta = 111·58°$, space group *C*2.

	Calculated			Experimental		
	x	*y*	*z*	*x*	*y*	*z*
Sr(1)	0·0940	0·0	0·2480	0·0873	0·0	0·2494
Sr(2)	0·2500	0·4802	0·2500	0·2455	0·4780	0·2458
Sr(3)	0·4021	−0.0407	0·2519	0·4128	−0·0207	0·2516
Si(1)	0·0	0·389	0·0	0·0	0·417	0·0
Si(2)	0·1262	0·780	0·015	0·116	0·790	−0·001
Si(3)	0·0	0·088	0·5	0·0	0·075	0·5
Si(4)	0·1262	0·679	0·485	0·130	0·702	0·498
O(1)	0·0	0·852	0·0	0·0	0·874	0·0
O(2)	−0·051	0·291	0·134	0·042	0·323	0·139
O(3)	0·106	0·550	0·006	0·107	0·532	−0·009
O(4)	0·123	0·822	−0·155	0·130	0·842	−0·142
O(5)	0·223	0·837	0·115	0·223	0·835	0·139
O(6)	0·0	0·621	0·5	0·0	0·605	0·5
O(7)	0·052	0·169	0·633	0·049	0·185	0·635
O(8)	0·099	0·910	0·494	0·110	0·911	0.511
O(9)	0·122	0·638	0·344	0·119	0·659	0·350
O(10)	0·223	0·622	0·614	0·213	0·643	0·630

(*b*) $Na_2BeSi_2O_9$
$a = 11·748$, $b = 9·415$, $c = 6·818$ Å, space group *Pnma*

	Calculated			Experimental		
	x	*y*	*z*	*x*	*y*	*z*
Na	0·66554	0·5341	−0·1562	0·65317	0·5331	−0·1522
Be	0·42264	0·0461	0·5946	0·43015	0·0600	0·5944
Si(1)	0·48311	0·25	−0·1090	0·49688	0·25	−0·0997
Si(2)	0·55865	0·25	0·3421	0·56241	0·25	0·3284
Si(3)	0·74736	0·25	0·0237	0·74559	0·25	0·0249
O(1)	0·47797	0·25	0·1379	0·47414	0·25	0·1403
O(2)	0·62572	0·25	−0·1070	0·63620	0·25	−0·1227
O(3)	0·68357	0·25	0·2331	0·69296	0·25	0·2496
O(4)	0·43115	0·1090	−0·1966	0·44696	0·1043	−0.1824
O(5)	0·53804	0·1087	0·4613	0·54057	0·1094	0·4533
O(6)	0·81793	0·1105	−0·0045	0·81267	0·1040	0·0013

Table 6. *A comparison of the calculated and experimentally determined fractional coordinates of the mineral beryl* ($Be_3Al_2Si_6O_{18}$) *which has six-membered silicate rings*

$a = 9·212$, $b = 9·236$ Å, space group *P*6/*mcc*.

		Calculated	Experimental
Be	*x*	0·5	0·5
	y	0·5	0·5
	z	0·75	0·75
Al	*x*	0·33333	0·33333
	y	0·66667	0·66667
	z	0·25	0·25
Si	*x*	0·3878	0·3892
	y	0·1249	0·1189
	z	0·0	0·0
O(1)	*x*	0·3199	0·3048
	y	0·2478	0·2352
	z	0·0	0·0
O(2)	*x*	0·5102	0·4983
	y	0·1473	0·1473
	z	0·1440	0·1445

calculations suggests that we could, in future studies, evaluate the structures of other actinide (*e.g.* Pa, Pu and Am) orthosilicates for which experimental determinations are not yet available.

3.2. *Ring silicates*

Silicates exist in many different ring configurations: the most common contain three or six linked tetrahedra. We have studied two three-membered-ring silicates, namely $Na_2Be_2Si_3O_9$ and α-$Sr_3Si_3O_9$ and one six-membered ring silicate, *i.e.* beryl, $Al_2Be_3Si_6O_{18}$. We should note that calculations on ring-structure silicates are more demanding than those based on isolated SiO_4 tetrahedra, as the former class contains two types of oxygen ions, namely bridging and non-bridging oxygens.

The $Na_2Be_2Si_3O_9$ structure is orthorhombic (Ginderow, Cesbron & Sichère, 1982) with Si_3O_9 rings parallel to (010). These rings are linked by Be_2O_6 groups which comprise two BeO_4 tetrahedra sharing one edge. The sodium ions occupy a seven-coordinate site within this framework. This compound was chosen because it has both sodium and beryllium ions present. Our other studies have included only alkaline-earth and transition metals. The calculation thus affords us the opportunity to test the reliability of the potential models for both Na^+ and Be^{2+}.

In the case of strontium silicate, the strontium–oxygen short-range parameters are almost certainly reliable, as they have been shown to reproduce crystal data on the oxide (Mackrodt & Stewart, 1979). Furthermore, a recent single-crystal study is available (Machida, Adachi, Shiokawa, Shimada & Koizumi, 1982). Discrepancies between experimental and calculated structures should provide a guide as to the adequacy of our potential model for the silicate ring.

The results on the three-membered system are summarized in Table 5. The starting configurations were based on ideal models with regular tetrahedra. They show that in both cases the calculated structure is in accord with experiment. The agreement for both are similar, suggesting not only that our Si···O potential is adequate for the ring-structure system, but also that the Be···O and Na···O potentials are acceptable.

The six-membered silicate-ring system beryl contains Al^{3+} in addition to Be^{2+}. The crystal structure of beryl was originally determined by Bragg & West (1926). A major problem is encountered in structural studies on this system in that at the centres of the silicate rings, particularly in natural samples, there are traces of water and alkali metals. The recent experimental determination (Hawthorne & Cerny, 1977) which we used for a comparison with the calculations had only very small traces of both. The good agreement achieved by our calculation (Table 6) suggests that any alkali metal or water present in this material does not significantly affect the structure.

C. Chain silicates. We considered three chain-structure silicates: firstly orthoenstatite, $MgSiO_3$; secondly, orthoferrosilite, $FeSiO_3$; and finally sodium metasilicate Na_2SiO_3.

Table 7. *The structure of enstatite* ($MgSiO_3$) *and ferrosilite* ($FeSiO_3$); *both have space group Pbca*

(*a*) $MgSiO_3$
$a = 18{\cdot}227,\ b = 8{\cdot}819,\ c = 5{\cdot}179$ Å

	Calculated			Experimental		
	x	*y*	*z*	*x*	*y*	*z*
Mg(1)	0·37624	0·66486	0·83336	0·37582	0·65379	0·86597
Mg(2)	0·38045	0·49564	0·32949	0·37677	0·48698	0·35897
Si(1)	0·27152	0·35106	−0·02496	0·27172	0·34162	0·05040
Si(2)	0·46675	0·34610	0·81062	0·47358	0·33734	0·79827
O*A*(1)	0·18348	0·34621	−0·00563	0·18343	0·34002	0·0346
O*B*(1)	0·55460	0·34960	0·84082	0·56236	0·34044	0·8000
O*A*(2)	0.31035	0.50940	0·02372	0·31094	0·50228	0·0433
O*B*(2)	0·42867	0·48098	0·66900	0·43283	0·48307	0·6893
O*A*(3)	0.29930	0·23754	0·74534	0·30313	0·22259	0·8319
O*B*(3)	0·44558	0·19624	0·61713	0·44764	0·19504	0·6036

(*b*) $FeSiO_3$
$a = 18{\cdot}427,\ b = 9{\cdot}076,\ c = 5{\cdot}237$ Å

	Calculated			Experimental		
	x	*y*	*z*	*x*	*y*	*z*
Fe(1)	0·37017	0·65392	0·96295	0·37574	0·65397	0·87456
Fe(2)	0·37643	0·41883	0·4278	0·37775	0·48566	0·3664
Si(1)	0·26109	0·3649	−0·0295	0·27231	0·3390	0·0494
Si(2)	0·49493	0·3561	0·8266	0·47315	0·3342	0·7893
O*A*(1)	0·18323	0·3577	0·0716	0·18490	0·3392	0·0384
O*B*(1)	0·5614	0·3553	1·0340	0·5610	0·3368	0·7859
O*A*(2)	0·2853	0·5092	0·1661	0·3120	0·4962	0·0575
O*B*(2)	0.4549	0·5199	0·7692	0·4330	0·4805	0·6922
O*A*(3)	0·2988	0·2704	−0·2682	0·3025	0·2355	−0·1832
O*B*(3)	0·4530	0·2517	0·5794	0·4475	0·2023	0·5871

The first two compounds have very similar structures. The two cations Mg^{2+} and Fe^{2+} occupy sixfold-coordinate sites and in both structures there are two types of silicate chains. There are three polymorphs of these materials, *i.e.* clino-, proto- and orthopyroxene. As discussed by Morimoto (1958) orthopyroxene can be regarded as composed of microscopically twinned layers of the clino structure; orthopyroxene is illustrated in Fig. 3. The magnesium and iron orthopyroxenes are the most stable configurations at room temperature.

As with the ring-structure compounds, the chain-structure silicates contain both bridging and non-bridging oxygen atoms. There has been much discussion (McDonald & Cruickshank, 1967; Cruickshank, 1961) as to the effect of covalence on these structures. It has been proposed that the oxygen ions which are involved in the bridging of the SiO_4 tetrahedra are more covalent because of the difference in π bonding between bridging and non-bridging ions. We might therefore expect that our simple potential models would be less capable of predicting the structure of the chain silicate $MgSiO_3$ (Sasaki and Takéuchi, 1982) than silicate minerals with separate SiO_4 tetrahedra. The results of our minimization studies summarized in Table 7 show that although there are larger discrepancies between the experimental and calculated structures for $MgSiO_3$ and $FeSiO_3$ than for the olivines, the discrepancies are still small, and the effects discussed above clearly do not have a major influence on the structures of these compounds.

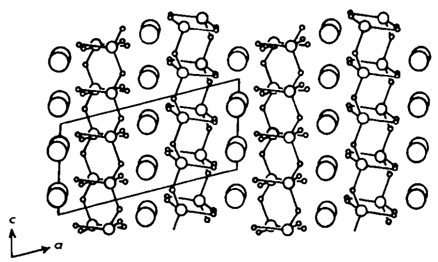

Fig. 3. The chain structure of orthopyroxene. Note pairs of silicate chains are superimposed.

Table 8. *The difference between experimentally determined and calculated fractional ionic coordinates for the chain silicate* Na_2SiO_3

Sodium metasilicate (Na_2SiO_3)
$a = 10{\cdot}482,\ b = 6{\cdot}064,\ c = 4{\cdot}826$ Å, space group *Cmc*2_1

		Calculated	Experimental
Na	*x*	0·17906	0·16562
	y	0·34535	0·33880
	z	0·00000	0·00000
Si	*x*	0·00000	0·00000
	y	0·17188	0·15737
	z	0·53059	0·53676
O(1)	*x*	0·12517	0·12947
	y	0·29810	0·28733
	z	0·47505	0·48105
O(2)	*x*	0·00000	0·00000
	y	0·06501	0·08436
	z	0·84995	0·87224

The crystal structure of sodium metasilicate was first determined by Grund & Pizy (1952). The structure was redetermined by McDonald & Cruickshank (1967) to confirm that there were two types of Si···O bonds. The silicate chains are parallel to the *c* axis and the bridging oxygen ions lie in the mirror plane. The sodium ions in this structure have fivefold coordination. The bridging Si···O bond has a mean length of 1·672 Å and non-bridging ones of 1·592 Å. McDonald & Cruickshank proposed that this large difference was due to *d–p* π bonding and suggested that the difference between the bridging and non-bridging oxygen ions required different bonding schemes for the two Si···O bonds.

The results of our energy-minimization studies in Table 8 show a remarkably good agreement with experiment. We predict the bridging Si···O bonds to have a mean length of 1·675 Å compared with 1·672 Å and non-bridging bond length to be 1·543 Å (*cf.* 1·592 Å). The differences are well within the uncertainties in the cell dimensions and thermal amplitudes. As discussed in § 2 we have only one type of oxygen ion in our potential model. Thus, the differences are due to other effects. Another postulated manifestation of the covalent bonding is the distortions of the bond angles from the ideal tetrahedral angle of 109°; in particular, the O–Si–O with bridging oxygen observed to be 103° and non-bridging 117°. But we calculate them as 98 and 116°, respectively. This suggests that covalency has the effect of reducing the distortions instead of increasing them.

3.3. *The effect of temperature and pressure on structures*

The results discussed above clearly encourage confidence in our potential models and simulation procedures. As a further test of the potential models, we will investigate, in this section, the extent to which static simulation techniques can be used to model, at least in part, the effects of temperature or pressure. The basis of our approach is the quasi-harmonic approximation, that is we simulate the effects of temperature and pressure by adjustment of the unit-cell dimensions. We then carry out an energy minimization with the modified cell dimensions. We considered two structural types for which relevant experimental data are available. The first is the garnet structure: here we studied the magnesium and calcium aluminosilicates. The second is olivine, including forsterite (Mg_2SiO_4) and fayalite (Fe_2SiO_4). All compounds contain isolated silicate tetrahedra.

The effect of pressure on the garnet-structure compounds is relevant because these minerals are thought to be an important constituent of the earth's interior, on the basis of their common occurrence in garnet peridotites and eclogites, and as experimental determinations have found them stable at high pressures.

As we have already seen, the structure of garnet is cubic and the cations occupy special sites; thus structural variations are confined to the oxygen sublattice (see Fig. 4). For both the magnesium and calcium garnets the positions of the oxygen sites were calculated for different unit-cell parameters, which were those determined experimentally (Hazen & Finger, 1978) for a range of pressures. The calculated and observed coordinates are given in Table 9 and a plot of the bond length *versus* pressure is given in Fig. 5. The graph shows that we can reproduce the main effects of pressure on the structure; in particular, we find that the Si···O bond distance does not vary with pressure. As expected, the best agreement is with the divalent cation–oxygen separation, because potential parameters describing the short-range interactions are most reliable for these interactions.

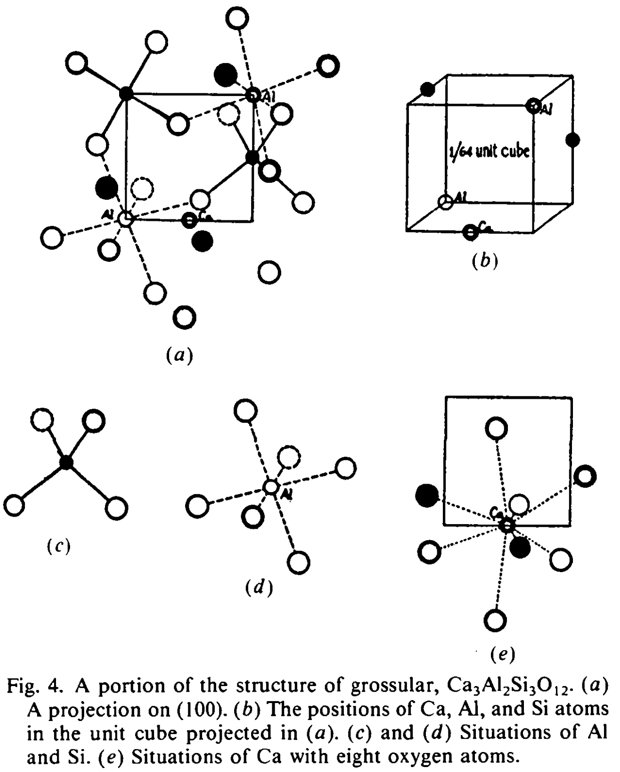

Fig. 4. A portion of the structure of grossular, $Ca_3Al_2Si_3O_{12}$. (*a*) A projection on (100). (*b*) The positions of Ca, Al, and Si atoms in the unit cube projected in (*a*). (*c*) and (*d*) Situations of Al and Si. (*e*) Situations of Ca with eight oxygen atoms.

Table 9. *The variation of oxygen parameters with pressure for two garnets*: $Mg_3Al_2Si_3O_{12}$ *and* $Ca_3Al_2Si_3O_{12}$

Pressure (GPa)	*a* (Å)		Experimental	Calculated
(*a*) $Mg_3Al_2Si_3O_{12}$				
10^{-4}	11·456	*x*	0·0328	0·0321
		y	0·0502	0·0364
		z	0·6534	0·6532
1·6	11·412	*x*	0·0329	0·0323
		y	0·0495	0·0372
		z	0·6532	0·6532
3·1	11·377	*x*	0·0327	0·0325
		y	0·0503	0·0380
		z	0·6522	0·6531
4·3	11·352	*x*	0·0331	0·0326
		y	0·0503	0·0385
		z	0·6532	0·6531
5·6	11·318	*x*	0·0313	0·0328
		y	0·0506	0·0391
		z	0·6535	0·6531
(*b*) $Ca_3Al_2Si_3O_{12}$				
10^{-4}	11·846	*x*	0·0380	0·0388
		y	0·0450	0·0340
		z	0·6518	0·6496
1·9	11·795	*x*	0·0372	0·0390
		y	0·0450	0·0345
		z	0·6516	0·6495
3·5	11·760	*x*	0·0379	0·0391
		y	0·0458	0·0349
		z	0·6518	0·6494
6·1	11·698	*x*	0·0359	0·0392
		y	0·0414	0·0356
		z	0·6496	0·6493

In our study of olivine structures, we investigated the effects of both temperature and pressure. The

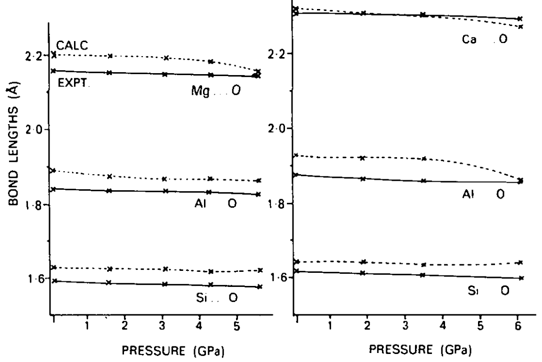

Fig. 5. The effects of pressure on the cation–oxygen bond lengths in two garnets. (i) Pyrope, (ii) grossular.

olivine structure, particularly forsterite (Mg_2SiO_4) is one of the most abundant minerals in the upper mantle. Thus, the effect of temperature and pressure changes on the structure could have important geochemical consequences, especially in the region where it transforms to the spinel structure.

We have described the structure in detail in § 3.1; Figs. 6(*a*) and 6(*b*) show the effect of pressure and temperature on the bond lengths. Our results agree with the experimental observations (Hazen, 1976, 1977), *i.e.* the variation in the Mg···O bond distance accounts for virtually all the response of the crystal to the change in volume. The octahedral distortions increase with temperature but do not otherwise show strong trends with increasing temperature.

4. Discussion and conclusions

The work described in the previous sections clearly establishes the capacity of the simulation techniques and potentials discussed in § 2 to reproduce accurately the observed structures of several classes of minerals given specified cell dimensions. The potential models used are of the simple ionic two-body form; and, although these are unquestionably an approximation when such models are applied to structure prediction in certain types of silicate, they do not appear to cause serious errors. In this context, two special features of potential models deserve comment. Firstly, we recall that our models omit Si···Si short-range interactions, which O'Keeffe & Hyde (1978) have argued were important in influencing the structures of a number of silicates. Although our work does not necessarily invalidate O'Keeffe's & Hyde's models, our results nevertheless show that there is no necessity for including these interactions. Secondly, we found that in the ring- and chain-structure silicates there was no need for using separate potential parameters for bridging and non-bridging oxygen ions. Arguments of McDonald & Cruickshank (1967) which are based on the considerable differences between the Si···O interactions for the two types of oxygen are not therefore supported by our results.

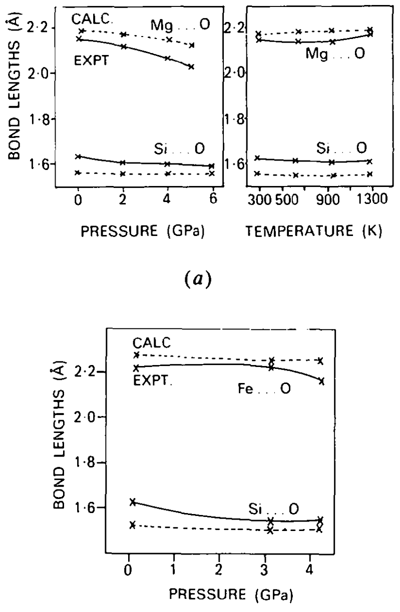

Fig. 6. (*a*) The effect of temperature and pressure on the cation–oxygen bond lengths in forsterite (Mg_2SiO_4). (*b*) The effect of pressure on bond lengths in fayalite (Fe_2SiO_4).

Despite the success of our study, it is important to bear in mind its limitations. Firstly, we should note that applications of the present potentials to framework-structured silicates have proved to be less successful; we believe that adequate results for these systems will require the inclusion of bond-bending forces in addition to the central force potentials used in the present models. Secondly, we should stress that, in the present calculation, the cell dimensions were held fixed at their experimentally observed values. As discussed in § 2, the restriction may be removed, at the cost of considerably greater computer time. Such calculations were performed for $ZrSiO_4$ and Na_2SiO_3. The results were encouraging in that changes in the cell dimensions were less than 2% when the experimental values were allowed to relax to their minimum-energy configuration; for work on compounds where both cell dimensions and atomic coordinates are unknown such calculations would clearly be of value.

In summary, our work establishes energy-minimization studies as a viable technique in structural studies of silicate minerals. Present potential models for these systems clearly contain a number of approximations; but they are sufficiently reliable for accurate predictions of the structures of at least certain classes of minerals.

SCP would like to thank SERC and AERE Harwell for financial support. We are also grateful to AERE and the University of London Computer Centre for the generous provision of computer time.

References

Baur, W. H. (1972). *Am. Mineral.* **57**, 709–712.
Bragg, W. L. & Brown, G. B. (1926). *Z. Kristallogr.* **63**, 538–556.
Bragg, W. L. & West, J. (1926). *Proc. R. Soc. London Ser. A*, **111**, 691–714.
Catlow, C. R. A. (1977). *Proc. R. Soc. London Ser. A*, **353**, 533–561.
Catlow, C. R. A., Cormack, A. N. & Theobald, F. (1984). *Acta Cryst.* **B40**, 195–200.
Catlow, C. R. A. & Mackrodt, W. C. (1982). *Computer Simulation of Solids. Lecture Notes in Physics*, Vol. 166. Berlin: Springer.

CATLOW, C. R. A. & STONEHAM, A. M. (1983). *J. Phys. C*, **16**, 4321–4338.

COCHRAN, W. (1961). *Nature (London)*, **191**, 60–61.

CRUICKSHANK, D. W. J. (1961). *J. Chem. Soc.* pp. 5486–5504.

FLETCHER, R. & REEVES, C. M. (1964). *Comput. J.* 7, 149–154.

FUCHS, L. H. & GEBERT, E. (1958). *Am. Mineral.* **43**, 243–247.

FUJINO, K., SASAKI, S., TAKÉUCHI, Y. & SADANAGA, R. (1981). *Acta Cryst.* **B37**, 513–518.

GIBBS, G. V. (1982). *Am. Mineral.* **67**, 421–450.

GINDEROW, D., CESBRON, F. & SICHÈRE, M. C. (1982). *Acta Cryst.* **B38**, 62–66.

GRUND, A. & PIZY, M. (1952). *Acta Cryst.* **5**, 837–840.

HAWTHORNE, F. C. & CERNY, P. (1977). *Can. Mineral.* **15**, 414–427.

HAZEN, R. M. (1976). *Am. Mineral.* **61**, 1280–1293.

HAZEN, R. M. (1977). *Am. Mineral.* **62**, 286–295.

HAZEN, R. M. & FINGER, L. W. (1978). *Am. Mineral.* **63**, 297–303.

HAZEN, R. M. & FINGER, L. W. (1979). *Am. Mineral.* **64**, 196–201.

JENKINS, H. B. D. (1982). In *Computer Simulation of Solids*, edited by C. R. A. CATLOW & W. C. MACKRODT. *Lecture Notes in Physics*, Vol. 166. Berlin: Springer.

JENKINS, H. B. D. & HARTMAN, P. (1979). *Philos. Trans. R. Soc. London Ser. A*, **293**, 169–180.

MCDONALD, W. S. & CRUICKSHANK, D. W. J. (1967). *Acta Cryst.* **22**, 37–43.

MACHIDA, K.-I., ADACHI, G.-Y., SHIOKAWA, J., SHIMADA, M. & KOIZUMI, M. (1982). *Acta Cryst.* **B38**, 386–389.

MAKRODT, W. C. & STEWART, R. F. (1979). *J. Phys. C*, **12**, 5015–5036.

MATSUI, M. & MATSUMOTO, T. (1982). *Acta Cryst.* **A38**, 513–515.

MIYAMOTO, M. & TAKEDA, H. (1980). *Geochem. J.* **14**, 243.

MORIMOTO, N. (1958). *Carnegie Inst. Washington Yearb.* **57**, 197–211.

NORGETT, M. J. & FLETCHER, R. (1970). *J. Phys. C*, **3**, 163–166.

O'KEEFFE, M. & HYDE, B. G. (1978). *Acta Cryst.* **B34**, 27–32.

PARKER, S. C. (1983). PhD Thesis. Univ. of London. Also available as UKAEA report AERE-TP968.

PAULING, L. (1980). *Am. Mineral.* **65**, 321–323.

SASAKI, S., FUJINO, K. & TAKÉUCHI, Y. (1979). *Proc. Jpn Acad. Ser. B*, **55**, 43–48.

SASAKI, S., FUJINO, K. TAKÉUCHI, Y. & SADANAGA, R. (1980). *Acta Cryst.* **A36**, 904–915.

SASAKI, S. & TAKÉUCHI, Y. (1982). *Z. Kristallogr.* **158**, 279–297.

SPEER, J. A. & COOPER, B. J. (1982). *Am. Mineral.* **67**, 804–809.

STEWART, R. F., WHITEHEAD, M. A. & DONNAY, G. (1980). *Am. Mineral.* **65**, 324–326.

TAYLOR, M. & EWING, R. C. (1978). *Acta Cryst.* **B34**, 1074–1079.

TOSSEL, J. A. (1977). *Am. Mineral.* **62**, 136–141.

Acta Cryst. (1984). **B40**, 208–213

Short-Range-Ordering in the Ba^{2+} Ion Distribution in Ba^{2+} β''-Alumina at 295 K

BY JOHN O. THOMAS AND MAGGIE ALDÉN

Institute of Chemistry, University of Uppsala, Box 531, *S*-751 21 *Uppsala, Sweden*

GARRY J. MCINTYRE

Institut Laue–Langevin, 156*X Centre de Tri,* 38042 *Grenoble, France*

AND GREGORY C. FARRINGTON

*Department of Materials Science and Engineering K*1, *University of Pennsylvania, Philadelphia, PA* 19104, *USA*

(*Received* 15 *September* 1983; *accepted* 15 *December* 1983)

Abstract

The Ba^{2+} ionic distribution in Ba^{2+} β''-alumina has been studied at 295 K by conventional single-crystal X-ray diffraction techniques (Mo $K\alpha$ radiation: $\lambda = 0{\cdot}710\,688$ Å). The structure [idealized formula $Ba_xMg_{2x-1}Al_{12-2x}O_{17}$ ($x = 5/6$), $M_r = 681{\cdot}5$, $F(000) = 972$] comprises a rhombohedral framework of spinel-type slabs separating the two-dimensional conduction planes with a spacing of ~11 Å. All atoms in the spinel skeleton appear to satisfy the centrosymmetric space group $R\bar{3}m$, with hexagonal cell dimensions: $a = 5{\cdot}619\,(1)$, $c = 34{\cdot}084\,(20)$ Å, $V = 932{\cdot}0\,(7)$ Å^3, $Z = 3$, $D_x = 3{\cdot}643\,(3)$ Mg m^{-3}, $\mu_{\rm calc} = 3{\cdot}61$ mm^{-1}. The arrangement of Ba^{2+} ions is found to be non-centrosymmetric at short-range, as evidenced by a distinct preference by the complete unit cell for the space group $R3m$. The Ba^{2+} ions occupy predominantly the 6(*c*) sites ($R\bar{3}m$ notation) with a mean ratio of ~3·5:1 between the refined occupations of adjacent sites. Significant Ba^{2+} density also lies on the conduction pathways between adjacent 6(*c*) sites. The column oxygen O(5) shows no significant displacement from the 3(*b*) site. The best fit to the data is obtained with third-rank cumulants (γ_{ijk}'s) describing the vibration of the Ba^{2+} ions. The effective formula is $Ba_{0{\cdot}82}Mg_{0{\cdot}63}Al_{10{\cdot}37}O_{17}$, assuming charge neutrality and charge compensation through Mg^{2+} substitution. The implications of the crystallographic result are discussed, particularly in connection with possible ionic conduction mechanisms.

0108-7681/84/030208-06$01.50